ELSEVIER

# Inclusions in diamonds from the K14 and K10 kimberlites, Buffalo Hills, Alberta, Canada: diamond growth in a plume?

Rondi M. Davies[a,*], William L. Griffin[a,b], Suzanne Y. O'Reilly[a], Tom E. McCandless[c]

[a] GEMOC ARC National Key Centre, School of Earth and Planetary Sciences, Macquarie University, Sydney, NSW 2109, Australia
[b] CSIRO Exploration and Mining, P.O. Box 136, North Ryde, NSW 1670, Australia
[c] Ashton Mining of Canada, Unit 123-930 West 1st Street, North Vancouver, BC, Canada VTP3N4

## Abstract

Analyses of mineral inclusions, carbon isotopes, nitrogen contents and nitrogen aggregation states in 29 diamonds from two Buffalo Hills kimberlites in northern Alberta, Canada were conducted. From 25 inclusion bearing diamonds, the following paragenetic abundances were found: peridotitic (48%), eclogitic (32%), eclogitic/websteritic (8%), websteritic (4%), ultradeep? (4%) and unknown (4%). Diamonds containing mineral inclusions of ferropericlase, and mixed eclogitic-asthenospheric-websteritic and eclogitic-websteritic mineral associations suggests the possibility of diamond growth over a range of depths and in a variety of mantle environments (lithosphere, asthenosphere and possibly lower mantle).

Eclogitic diamonds have a broad range of C-isotopic composition ($\delta^{13}C = -21‰$ to $-5‰$). Peridotitic, websteritic and ultradeep diamonds have typical mantle C-isotope values ($\delta^{13}C = -4.9‰$ av.), except for two $^{13}C$-depleted peridotitic ($\delta^{13}C = -11.8‰$, $-14.6‰$) and one $^{13}C$-depleted websteritic diamond ($\delta^{13}C = -11.9‰$). Infrared spectra from 29 diamonds identified two diamond groups: 75% are nitrogen-free (Type II) or have fully aggregated nitrogen defects (Type IaB) with platelet degradation and low to moderate nitrogen contents (av. 330 ppm-N); 25% have lower nitrogen aggregation states and higher nitrogen contents ($\sim 30\%$ IaB; $< 1600$ ppm-N).

The combined evidence suggests two generations of diamond growth. Type II and Type IaB diamonds with ultradeep, peridotitic, eclogitic and websteritic inclusions crystallised from eclogitic and peridotitic rocks while moving in a dynamic environment from the asthenosphere and possibly the lower mantle to the base of the lithosphere. Mechanisms for diamond movement through the mantle could be by mantle convection, or an ascending plume. The interaction of partial melts with eclogitic and peridotitic lithologies may have produced the intermediate websteritic inclusion compositions, and can explain diamonds of mixed parageneses, and the overlap in C-isotope values between parageneses. Strong deformation and extremely high nitrogen aggregation states in some diamonds may indicate high mantle storage temperatures and strain in the diamond growth environment. A second diamond group, with Type IaA–IaB nitrogen aggregation and peridotitic inclusions, crystallised at the base of the cratonic lithosphere. All diamonds were subsequently sampled by kimberlites and transported to the Earth's surface.

* Corresponding author. Present address: Department of Earth and Planetary Sciences, American Museum of Natural History, New York, NY 10024-5192, USA. Tel.: +1-212-769-5314; fax: +1-212-769-5339.
E-mail address: rdavies@amnh.org (R.M. Davies).

## 1. Introduction

Syngenetic mineral inclusions trapped in diamond represent pristine samples of mantle material incorporated in the diamond during its growth. Such inclusions provide direct evidence of the composition and physical conditions of ancient mantle and diamond growth environments, and allow us to place constraints on the tectonic histories of the diamond-bearing mantle beneath cratons. Diamond inclusion studies can also be applied to diamond exploration by identifying minerals of characteristic compositions that can be targeted as prospective indicators.

Diamond morphology (including surface resorption and deformation features), C-isotopes, defect and impurity abundances (mainly nitrogen) measured by FTIR spectroscopy provide additional evidence that can shed light on the origins of diamond; through identifying the origin of the carbon and the conditions of diamond growth, mantle storage and emplacement.

This paper reports the results of a study of 29 diamonds, 25 of which syngenetic inclusions were extracted and analysed, from the Buffalo Hills K14 (24) and K10 (1) kimberlite pipes in Alberta, Canada. An additional 10 diamonds have been analysed for C-isotopes. The results provide evidence that the diamonds have a complex mantle evolutionary history having grown in changing chemical environments of the lower mantle, asthenospheric and lithospheric mantle.

## 2. Geological setting

The Buffalo Hills kimberlite field, comprising 36 kimberlites discovered to date, occurs within the Precambrian Buffalo Head Terrane of northern Alberta, Canada (Ross et al., 1991; Carlson et al., 1998; McNicoll et al., 2000; Ross, 2002; Fig. 1). The terrane has no surface exposure, and is overlain by a thick sequence of Devonian and Cretaceous sedimentary rocks through which the Cretaceous kimberlites have erupted. Sm–Nd and U–Pb ages suggest the terrane formed between 2.3 and 2.0 Ga (Ross et al., 1991; Villeneuve et al., 1993; McNicoll et al., 2000). Bounded by the structural discontinuities of the Great Slave Lake shear zone to the north, the Snowbird Tectonic Zone to the south and the Taltson plutonic
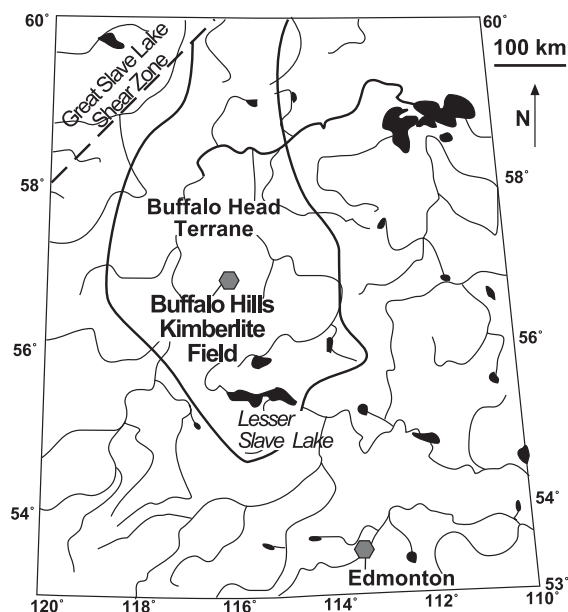


Fig. 1. Locality map of the Buffalo Head terrane with the Buffalo Hills Kimberlite Field shaded (modified from Carlson et al., 1998).

belt to the east, the Buffalo Head Terrane is thought to represent a crustal sliver that was incorporated with other Archean and Proterozoic crustal blocks through subduction, accretion and orogenesis around 2.0 Ga.

## 3. Samples and analytical techniques

The morphological features of 29 diamonds starting with Ash- are described (Table 1) and mineral inclusions identified prior to diamond crushing. The 10 diamonds with sample numbers starting with BH- are only considered in the C-isotope section of this paper. From 25 of the 29 diamonds, 53 crystalline inclusions were extracted (Table 2). Fifteen diamonds also contained epigenetic phases (Table 2). Crystalline inclusions were identified prior to destruction of the sample by the absence of cracks around the inclusion, by their geometric shapes, and by their unaltered appearance once extracted. Mineral inclusions are between 20 and 200 μm across. Epigenetic inclusions are typically larger (≤400 μm across).

The mineral inclusions were extracted by breaking individual diamonds in a closed cell in a custom-built stainless steel vice with a tungsten carbide piston.

Table 1
Syngenetic inclusion parageneses, morphological characteristics, carbon isotopes and nitrogen characteristics diamonds from the K14 kimberlite

| Sample | Weight (g) | Col. | Shape | RC | Defm | Abr. | Para. | Inclusions | $\delta^{13}C$ | N (ppm) | % IaB | Comments |
|---|---|---|---|---|---|---|---|---|---|---|---|---|
| Ash-101 | 0.0057 | C-l | D F | 1 | | – | P | Fo | − 4.7 | 750 | 100 | H, no P |
| Ash-102A | 0.0244 | C-l | D | 1 | | | E | Gnt | − 18.8 | 450 | 100 | H, no P |
| Ash-102B | 0.008 | Y | D | 1 | | – | P | Fo | − 5.0 | 1620 | 20 | H |
| Ash-104A | 0.0061 | B | E D | 1 | LL, Sh, Btl | – | P | Fo (3), cpx | − 11.8 | 0 | 0 | Type II |
| Ash-104B | 0.0138 | B | D F | 1 | LL, Sh | – | P | Fo | − 4.7 | 0 | 0 | Type II |
| Ash-104C | 0.0184 | B | D Ag | 1 | LL, Sh | – | – | – | − 2.9 | < 50 | 100 | H, no P |
| Ash-105A | 0.0122 | C-l | D | 3 | LL, Sh, Btl | – | E | Majorite (2) | − 14.8 | 0 | 0 | Type II |
| Ash-105B | 0.0174 | B | D Tw F | 1 | LL | – | P | Fo | − 3.6 | 0 | 0 | Type II |
| Ash-105pm | 0.0027 | B | D F | 1 | Sh | – | P | Gnt, Fo | − 2.7 | < 50 | 100 | H, no P |
| Ash-106A | 0.0176 | C-l | D Tw | 3 | | – | E? | Fe-Gnt | − 6.9 | 720 | ~ 30 | Type I |
| Ash-106B | 0.0196 | pY | D | 1 | | – | – | – | − 5.6 | [a] | [a] | Type I |
| Ash-106C | 0.0061 | Y | D Tw | 1 | LL, Sh | – | P | Fo | − 6.4 | 900 | 15 | H |
| Ash-106D | 0.0031 | C-l | D Tw | 1 | | – | P | Cr-sp (>10) | − 2.7 | 0 | 0 | Type II |
| Ash-106pm | 0.0084 | B | D F | 1 | Sh | – | P | Fo | − 14.6 | 230 | 100 | H, no P |
| Ash-108A | 0.0576 | B | D F | 2 | LL, Sh, Btl | bf | E | Gnt | − 4.8 | 65 | 100 | H, no P |
| Ash-108B | 0.0013 | B | D Tw F | – | | – | E/W | Gnt-cpx-ru, Gnt (2), E-cpx (2), W-cpx, Maj | − 4.8 | 0 | 0 | Type II |
| Ash-109A | 0.003 | pB | D F | 1 | Sh | – | UD | fPer | − 4.6 | 0 | 0 | Type II |
| Ash-109pm | 0.0031 | C-l | D | 1 | | – | Web | Cpx | − 11.9 | 830 | 100 | H, no P |
| Ash-110 | 0.0067 | C-l | D Tw | 1 | Sh | – | P | Cpx | − 8.8 | 0 | 0 | Type II |
| Ash-111A | 0.0216 | C-l | D Tw | 1 | | – | – | – | − 5.8 | 1070 | < 10 | no P, H |
| Ash-111B | 0.0127 | C-l | D F | 1 | | – | E | Ru | − 4.7 | 0 | 0 | Type II |
| Ash-111C | 0.0082 | B | F D | 1 | Btl, Sh | – | E | Gnt | − 14.6 | 0 | 0 | Type II |
| Ash-111D | 0.0073 | C-l | F O | 4 | LL, Sh, Btl | bf | E | Cpx (2) | − 14.7 | 0 | 0 | Type II |
| Ash-111E | 0.0053 | pB | D Tw | 1 | Sh | – | – | – | − 3.7 | 0 | 0 | Type II |
| Ash-111F | 0.0036 | B | D F | 2 | LL, Sh, Btl | – | E | Cpx | − 20.6 | [a] | [a] | Type I |
| Ash-111G | 0.0023 | C-l | Ir D F | 2 | LL, Sh, Btl | – | E | Cpx | − 13.7 | 400 | 100 | H, no P |
| Ash-111H | 0.0363 | pB | D F | 1 | LL, Sh, Btl | bf | E/W | Cpx (>3) | − 4.6 | 135 | 100 | H, no P |
| Ash-113 | 0.0051 | pB | Ir D | 1 | LL, Sh, Btl | – | P | Fo (2) | − 5.7 | 560 | 12 | P |
| Ash-K10-2 | 0.0019 | C-l | O Tw | 5 | | – | P | Gnt, Fo (8) Cpx (3), | − 3.8 | 0 | 0 | Type II |
| BH14-1 | 0.0041 | C-l | D Ag | 1 | | | | | − 7.2 | – | – | |
| BH14-2 | 0.0023 | C-l | O F | 4 | | bf | | | − 4.9 | – | – | – |
| BH14-3 | 0.0041 | C-l | O F | 4 | | bf | | | − 6.1 | – | – | – |
| BH14-4 | 0.0012 | C-l | O | 5 | | | | | − 3.5 | – | – | |
| BH14-5 | 0.0031 | pB | C F | 4 | | bf | | | − 2.6 | – | – | – |
| BH14-6 | 0.0023 | C-l | F | 1 | | bf | | | − 4.1 | – | – | – |
| BH14-7 | 0.0023 | C-l | F | 2 | | bf | | | − 7.1 | – | – | – |
| BH14-8 | 0.0046 | C-l | F Ir | 1 | | bf | | | − 12.0 | – | – | – |
| BH14-9 | 0.0008 | C-l | F | 1 | | bf | | | − 3.9 | – | – | – |
| BH14-10 | 0.0012 | C-l | C-O F | 3 | | bf | | | − 6.4 | – | – | – |

Col. = colour, C-l = colourless, B = brown, Y = yellow, p = pale, D = dodecahedron, O = octahedron, E = elongate, Ag = aggregate, Tw = twinned, F = fragment, Ir = irregular, RC = resorption class (Robinson et al., 1989), LL = lamination lines, Sh = shagreen texture, Btl. = brittle displacement laminae, Defm = deformation, Abr. = abrasion, bf = broken face, Para = paragenesis, E = eclogitic, P = peridotitic, Web = websteritic, UD = ultradeep, Gnt = garnet, Cpx = clinopyroxene, Fo = olivine, Ru = rutile, Cr. sp. = Cr-spinel, Maj = majoritic garnet, fPer = ferropericlase. P = platelets, H = hydrogen.

[a] Data unresolved due to poor quality spectra.

Following crushing, the diamond rubble was tipped into a petrie dish and inclusions were identified using binocular and petrographic microscopes. Inclusions were then individually placed in petropoxy resin 154 on a glass slide. The epoxy was heat-hardened at 200 °C for 15 min. The inclusions in epoxy were polished by hand using fine wet and dry sandpaper and diamond paste.

Table 2
Inclusion abundances in diamonds from the K10 and K14 kimberlites, Alberta, Canada

| Para. | Single phases | $n$ | Para. | Multiple phases | $n$ | Secondary phases | |
|---|---|---|---|---|---|---|---|
| E | Gnt | 3 | P | Gnt, Fo (not recovered) | 1 | Sphene + serpentine | 1 |
| E | Maj | 1 | P | Fo-Cr. diop-Gnt | 1 | Carbonate | 7 |
| E | Rutile | 1 | P | Fo-Cr. diop | 1 | Perovskite | 2 |
| E? | Fe-gnt | 1 | P | Cr-diop-serpentine | 1 | Phlogopite | 1 |
| E | Cpx | 3 | E-Web | Gnt-E. cpx-Ru, Maj, | 2 | Phlogopite-carbonate-perovskite | 2 |
| Web | Cpx | 1 | | W. cpx, E. Cpx | | Serpentine | 2 |
| P | Fo | 7 | | | | | |
| P | Cr-sp. | 1 | | | | | |
| UD | fPer | 1 | | | | | |
| Total | | 19 | | | 6 | | 15 |

Major-element compositions of mineral inclusions were analysed using a Cameca SX 50 electron micro-probe at Macquarie University. Operating conditions included an accelerating voltage of 15 kV, a sample current of 20 nA and a beam width about 3 μm, with a mixture of natural and synthetic minerals standards. Minor and trace elements in garnet inclusions were determined by laser ablation ICP-MS using a Perkin-Elmer Sciex ELAN 6000 coupled with a 266nm Nd:YAG laser at Macquarie University. The NIST 610 glass standard was used for calibration of element sensitivities and Ca determined by electron probe was used as an internal standard. Analytical techniques, accuracy and precision are discussed in detail by Norman et al. (1996, 1998).

Carbon isotope analyses for diamonds with sample numbers starting with Ash- were carried out at the Centre for Isotope Studies, CSIRO, North Ryde. Fragments of diamond weighing ~ 1 mg were placed into a baked clean quartz glass tube with 10–20 mg of conditioned CuO agent. Tubes were evacuated, sealed and reacted in a furnace at 1000 °C for 5 h. $CO_2$ was collected in a gas sample tube for mass spectrometric analysis (Finnigan 252 mass spectrometer using dual inlet mode). An anthracite standard ($\delta^{13}C = -23.1\%o$) was run with most

batches and international graphite standard NBS21 ($\delta^{13}C = -28.1\%o$) was analysed at regular intervals. Carbon isotope analyses of the 10 diamonds with sample numbers beginning with BH- were contracted by Ashton Mining of Canada.

Fourier-transform-infrared spectra of diamonds were measured using a Digilab BIO-RAD FTS-60A attached to a UMA 300A IR-microscope with a liquid nitrogen reservoir at the Division of Coal and Energy Technology, North Ryde. Spectra were measured between wave numbers of 4400 and 550 cm$^{-1}$. The beam aperture was ≈ 90 μm. Sixty-four scans were made per analysis at a resolution of 8 cm$^{-1}$. Nitrogen contents in diamond were calculated from the spectra using the methods outlined in Mendelssohn and Milledge (1995). Nitrogen calculations assume pure IaA and IaB defects equal 160 and 750 at. ppm, respectively, at a fixed absorption coefficient of 1 per mm for diamond of 1 mm thickness (Woods et al., 1990; Mendelssohn and Milledge, 1995).

## 4. Diamond characteristics

Twelve of the twenty-nine diamonds are colourless, fourteen are brown and three are yellow. Twenty-seven diamonds are strongly resorbed octahedra (dodecahedra) and two are octahedra. Nine of the twenty-nine diamonds are twinned, one is an aggregate and eleven are fragments.

Common surface features on dodecahedral faces include large and small hillocks, polished low-relief surfaces, dissolution laminae and resorbed plates. Four diamonds have well-defined faces and edges. Eleven diamonds have freshly broken faces; fracturing may have occurred during extraction of the diamond from its host rock. Octahedral surfaces are planar and host negative trigonal and hexagonal etch pits. Etch channels (ruts) are prevalent (21%) and are commonly filled with serpentine.

Deformation is evident on the surfaces of two-thirds of the 29 diamonds. Nine of the diamonds with evidence of deformation show plastic deformation features with lamination lines and shagreen textures (micro-hillocks indicating the intersection of two or more sets of lamination lines). The other nine show both plastic and brittle deformation with displacements along slip planes expressed as steplike linea-

tions with herringbone textures, indicating stronger deformation during their growth and/or mantle storage. Most of the nondeformed diamonds are colourless, whereas 13 of the 18 deformed diamonds are shades of brown. This observation supports other studies, which have observed that brown colouration is prevalent in deformed diamond (e.g., Robinson et al., 1989).

## 5. Mineral inclusions in diamonds

### 5.1. Eclogitic garnet

Nine low-Cr garnets were extracted and analysed from five diamonds (Table 3). Except for the inclusion in diamond 106A, compositions are within the range of eclogitic inclusions worldwide with moderate contents of Fe, Mg and Ca (Mg# ($100Mg/(Mg+Fe_{Total})$)) 44 to 57; XCa ($100Ca/(Ca+Fe+Mg)$) 21 to 30). Three garnets in two eclogitic diamonds (105A, 108B) are moderately majoritic (garnet and clinopyr-

oxene in solid solution). One of these diamonds (108B) also contains two normal garnet inclusions, one of which is in contact with clinopyroxene and a rutile, and three clinopyroxenes.

The three majoritic garnets are characterised by excess Si (3.12–3.19 cations per formula unit (pfu) for 12 oxygens) at the expense of Al, which falls below the ideal value of 2 (1.56 to 1.72 cations pfu; Fig. 2a). The majoritic garnet inclusions have very high Na (0.22–0.23) and Ti (0.072–0.093; Fig. 2b) and higher Ca and lower Mg and Fe contents than other garnet inclusions. Elemental relationships may be explained by the high-pressure coupled substitution of $Si^{4+}-Na^{+}$ for $Al^{3+}-Mg^{2+}$ as shown in experiments by Irifune et al. (1986), with compositions corresponding to experimentally calibrated maximum pressures of formation of about 9 GPa (Fig. 2a). Such pressures correspond to asthenospheric depths of about 275 km.

Na and Ti contents in the Buffalo Hills eclogitic garnet diamond inclusions are high and show a bimodal distribution corresponding to the majoritic

Table 3
Representative electron microprobe analyses of eclogitic and peridotitic garnet inclusions in diamond

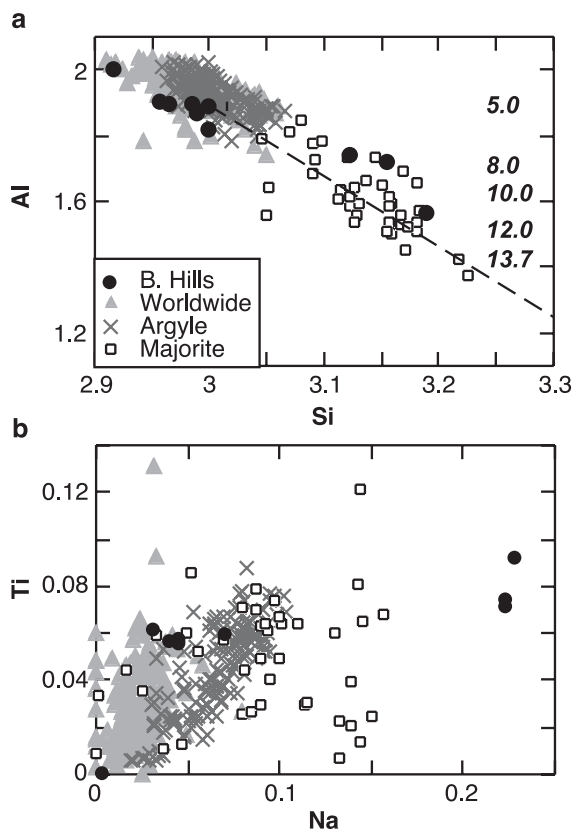| Sample | 106A | 102A | 105A(1) | 105A(2) | 108A | 108B(1) | 108B(2) | 108B(3) | 111C | K10 | 105C |
|---|---|---|---|---|---|---|---|---|---|---|---|
| Mineral | Alm-gt | Gt | Maj | Maj | Gt | Maj | Gt | Gt | Gt | Gt | Gt |
| Para. | E | E | E | E | E | E | E | E cpx-gt | E | P | P |
| Assoc. Anal. | 4 | 4 | 3 | 3 | 5 | 6 | 3 | 4 | 4 | 3 | 3 |
| $SiO_2$ | 35.7 | 39.8 | 42.2 | 41.5 | 40.1 | 42.4 | 39.9 | 39.4 | 39.4 | 41.0 | 41.6 |
| $TiO_2$ | 0.02 | 1.01 | 1.28 | 1.33 | 1.10 | 1.64 | 1.00 | 1.01 | 1.06 | 0.21 | 0.05 |
| $Al_2O_3$ | 20.8 | 21.4 | 19.5 | 19.6 | 20.7 | 17.6 | 21.1 | 21.4 | 21.1 | 17.7 | 16.7 |
| $Cr_2O_3$ | <0.06 | <0.06 | 0.07 | <0.06 | <0.06 | 0.08 | <0.06 | <0.06 | <0.06 | 7.02 | 7.89 |
| FeO | 32.0 | 16.58 | 14.49 | 14.44 | 16.92 | 14.72 | 16.60 | 16.66 | 18.28 | 6.62 | 7.17 |
| MnO | 6.67 | 0.29 | 0.31 | 0.28 | 0.40 | 0.26 | 0.29 | 0.28 | 0.42 | 0.17 | 0.28 |
| MgO | 3.87 | 10.86 | 9.54 | 9.63 | 12.42 | 10.39 | 11.04 | 10.87 | 8.10 | 20.34 | 19.93 |
| CaO | 0.46 | 9.73 | 10.66 | 10.82 | 8.16 | 10.69 | 9.86 | 9.93 | 11.06 | 5.76 | 6.06 |
| $Na_2O$ | 0.02 | 0.28 | 1.55 | 1.53 | 0.21 | 1.57 | 0.31 | 0.32 | 0.48 | 0.02 | 0.01 |
| $K_2O$ | <0.04 | <0.04 | <0.04 | <0.04 | <0.04 | <0.04 | <0.04 | <0.04 | <0.04 | <0.04 | <0.04 |
| NiO | <0.06 | <0.06 | <0.06 | <0.06 | <0.06 | <0.06 | <0.06 | <0.06 | <0.06 | <0.06 | <0.06 |
| Total [12O] | 99.7 | 100.0 | 99.7 | 99.2 | 100.0 | 99.6 | 100.1 | 100.0 | 99.9 | 98.9 | 99.7 |
| Si | 2.916 | 2.984 | 3.155 | 3.122 | 3.000 | 3.188 | 2.989 | 2.964 | 2.999 | 2.998 | 3.032 |
| Al | 2.004 | 1.893 | 1.721 | 1.741 | 1.822 | 1.564 | 1.865 | 1.895 | 1.888 | 1.524 | 1.434 |
| Ti | 0.001 | 0.057 | 0.072 | 0.075 | 0.062 | 0.093 | 0.056 | 0.057 | 0.060 | 0.011 | 0.003 |
| Na | 0.004 | 0.041 | 0.224 | 0.224 | 0.031 | 0.228 | 0.045 | 0.046 | 0.071 | 0.002 | 0.001 |
| Mg# | 17.7 | 53.9 | 54.0 | 54.3 | 56.7 | 55.7 | 54.2 | 53.8 | 44.1 | 84.6 | 83.2 |
| XCa | 0.01 | 0.26 | 0.30 | 0.30 | 0.21 | 0.29 | 0.26 | 0.26 | 0.30 | 0.15 | 0.15 |
| XMg | 0.15 | 0.40 | 0.38 | 0.38 | 0.45 | 0.39 | 0.40 | 0.40 | 0.31 | 0.72 | 0.70 |
| XFe | 0.69 | 0.34 | 0.32 | 0.32 | 0.34 | 0.31 | 0.34 | 0.34 | 0.39 | 0.13 | 0.14 |
| XMn | 0.15 | | | | | | | | | | |

Fig. 2. Cation ratios (for 12 oxygen atoms) of eclogitic garnet inclusions in the Buffalo Hills diamonds and other diamond inclusions worldwide. The Argyle inclusion data are from Hall and Smith (1984), Sobolev et al. (1986) and Moore et al. (1989). In (a), numbers indicate pressure in GPa from which garnet with these Si/Al ratios are synthesised from pyrolite minus olivine (Irifune et al., 1986).



Fig. 3. Chondrite normalised rare earth element abundances of eclogitic garnet inclusions.

La, creating a sinusoidal LREE pattern. The majoritic garnet inclusion has lower REE, Zr and Hf and higher Ti than the other garnet inclusions. All inclusions show significant negative anomalies in Sr, Ga and V (Table 4).

The concave REE pattern for the majoritic garnet suggests a complex history of melt depletion (deple-

and normal garnet groups (Fig. 2b). Garnets show values similar to those in the Argyle diamonds from Western Australia that also occur in Proterozoic mantle (Jaques et al., 1989). High Na and Ti may indicate both high-pressure formation (e.g., McCandless and Gurney, 1989) and/or an Na- and Ti-rich eclogite bulk composition.

The trace element patterns of six eclogitic garnet inclusions from four diamonds are relatively flat, with heavy rare earth element (HREE) enrichment in two diamonds (108A, 111C) and HREE depletion in the others (Fig. 3). In all but one inclusion (the majoritic garnet from 108B), light rare earth elements (LREE) Ce, Pr and Nd are depleted except for

Table 4
Trace element abundances in eclogitic garnet inclusions from Buffalo Hills diamonds

| Sample | 102A | 108A | 108B(1) | 108BMaj | 111C | Average |
|---|---|---|---|---|---|---|
| U | 31.5 | 43.2 | 24.7 | – | 38.3 | 34.4 |
| Th | 57.0 | 38.3 | 36.4 | – | 64.6 | 49.1 |
| Sr | 1.51 | 1.71 | 1.23 | 1.04 | 5.74 | 2.25 |
| La | 16.62 | 12.36 | 11.93 | 0.47 | 20.5 | 12.36 |
| Ce | 10.28 | 9.37 | 7.46 | 2.50 | 13.43 | 8.61 |
| Pr | 9.15 | 8.36 | 7.52 | 5.16 | 14.25 | 8.89 |
| Nd | 11.60 | 8.51 | 9.73 | 9.06 | 29.6 | 13.70 |
| Sm | 21.8 | 12.6 | 23.1 | 17.00 | 40.8 | 23.1 |
| Eu | 23.9 | 13.3 | 28.0 | 19.64 | 32.1 | 23.4 |
| Gd | 21.6 | 15.0 | 22.9 | 16.79 | 31.5 | 21.6 |
| Dy | 16.48 | 20.0 | 17.31 | 13.19 | 28.0 | 18.99 |
| Ho | 12.68 | 20.0 | 14.03 | 10.97 | 25.2 | 16.58 |
| Y | 11.92 | 19.55 | 11.92 | 9.36 | 24.1 | 15.37 |
| Er | 11.33 | 22.7 | 11.33 | 8.18 | 25.2 | 15.73 |
| Yb | 9.85 | 29.5 | 10.46 | 6.52 | 27.7 | 16.81 |
| Lu | 10.29 | 29.6 | 9.88 | 7.00 | 23.9 | 16.13 |
| Sc | 4.74 | 12.18 | 4.91 | 4.43 | 7.90 | 6.84 |
| Ga | 1.19 | 1.18 | 0.98 | 0.90 | 1.09 | 1.07 |
| Zr | 36.0 | 31.5 | 28.0 | 11.17 | 38.1 | 29.0 |
| Hf | 33.7 | 37.0 | 26.0 | 11.44 | 38.5 | 29.3 |
| Ti | 12.71 | 14.70 | 12.30 | 20.6 | 11.55 | 14.36 |
| V | 1.15 | 4.66 | 1.22 | 2.06 | 2.94 | 2.41 |
| Nb | 5.53 | 24.8 | 0.69 | 14.23 | 5.61 | 10.17 |
| Ta | 21.8 | 7.75 | 4.93 | 14.08 | 16.20 | 12.96 |

tion of LREE) with subsequent metasomatic enrichment of the MREE (Griffin et al., 1999 and references therein). The enrichment in La and Ce in the normal garnet inclusions is unusual and distinctive from the eclogitic majoritic garnet and implies a complex history for the eclogite protolith.

A crystalline almandine-rich garnet (32.0 wt.% FeO) with high Mn (6.67 wt.%) and no Na was found in one diamond (analysis 106A; Table 3). Although it is unlikely that the extraction methodology used could account for contamination, the inclusion had not been identified prior to the destruction of the diamond so it is considered with caution. We cannot rule out the possibility that the inclusion may have been embedded in a rut or crack on the diamond's surface. However, the diamond contained a large graphite rosette, which could be where the inclusion resided.

### 5.2. Peridotitic garnet

Two chrome-pyrope garnets were analysed from two diamonds (105C and K10, Table 3). Based on their low ratios of $Cr_2O_3$ (7.0 and 7.9 wt.%) to CaO (5.8 and 6.1 wt.%), and the coexistence of one inclusion with chrome-diopside and relatively Fe-rich olivine (Fo 90–91), the garnets are classified as lherzolitic.

### 5.3. Clinopyroxene

Sixteen inclusions were extracted from nine diamonds. Thirteen representative analyses are shown in Table 5. The compositions of the clinopyroxene inclusions show a continuum from Cr-diopside with peridotitic affinity (0.60–1.48 wt.% $Cr_2O_3$; Mg# = 93) to intermediary clinopyroxene compositions with lower $Cr_2O_3$ (0.20–0.48 wt.%; Mg# = 74–87) and moderate jadeite (≤21 mol% Jd), to eclogitic compositions (<0.05–0.09 wt.% $Cr_2O_3$; 26–35 mol% Jd; Mg# = 76–89; Fig. 4a and b). The intermediary clinopyroxene compositions containing both Cr and jadeite share characteristics with peridotitic and eclogitic diamond inclusions and here are classified as websteritic. The eclogitic and websteritic clinopyroxenes both are distinguished from the peridotitic ones by higher Ti contents (Fig. 4c).

Four websteritic clinopyroxenes occur in three diamonds (108B, 109P, 111H). 108B also contains eclogitic clinopyroxene, garnet and majoritic garnet. This may suggest a compositional variation in the bulk chemistry of rocks encasing diamond through time with inclusions trapped at different stages in the diamonds growth history. Alternatively the variable clinopyroxene compositions in diamonds 108B and

Table 5

Representative electron microprobe analyses of eclogitic, websteritic and peridotitic clinopyroxene inclusions in diamond

| Sample | 110 | 104A | 108B-1 | 108B-2 | 108B-3 | 109P | 111D-1 | 111D-2 | 111F | 111G | 111H-1 | 111H-2 | K10 |
|---|---|---|---|---|---|---|---|---|---|---|---|---|---|
| Para. | P | P | E | E | Web | Web | E | E | E | E | Web | Web | P |
| Anal. | 3 | 3 | 3 | 3 | 3 | 4 | 2 | 3 | 3 | 3 | 3 | 5 | 3 |
| $SiO_2$ | 55.0 | 55.0 | 54.7 | 55.1 | 54.7 | 48.4 | 56.4 | 55.6 | 53.6 | 54.3 | 54.2 | 52.8 | 55.2 |
| $TiO_2$ | 0.03 | 0.05 | 0.81 | 0.80 | 0.62 | 1.60 | 0.29 | 0.40 | 0.16 | 0.21 | 0.60 | 0.20 | <0.03 |
| $Al_2O_3$ | 1.02 | 0.74 | 8.61 | 8.71 | 4.81 | 3.79 | 6.40 | 5.71 | 7.49 | 7.38 | 4.79 | 0.78 | 1.04 |
| $Cr_2O_3$ | 1.48 | 0.64 | 0.06 | 0.05 | 0.22 | 0.34 | 0.05 | 0.09 | <0.05 | <0.05 | 0.20 | 0.48 | 1.08 |
| FeO | 2.39 | 2.73 | 4.97 | 5.18 | 7.26 | 7.38 | 3.11 | 5.56 | 5.83 | 6.05 | 7.34 | 4.36 | 2.34 |
| MnO | <0.05 | 0.12 | <0.05 | <0.05 | 0.07 | 0.12 | 0.08 | 0.10 | 0.06 | 0.06 | 0.08 | 0.06 | 0.06 |
| MgO | 17.28 | 18.51 | 9.83 | 9.66 | 11.98 | 13.99 | 13.62 | 12.76 | 10.36 | 10.46 | 11.91 | 16.69 | 17.49 |
| CaO | 21.1 | 20.9 | 13.97 | 13.79 | 16.57 | 22.3 | 16.27 | 14.88 | 17.55 | 17.46 | 16.51 | 22.4 | 22.1 |
| $Na_2O$ | 1.11 | 0.74 | 6.01 | 6.09 | 3.34 | 0.40 | 3.86 | 3.86 | 3.74 | 3.69 | 3.31 | 0.59 | 0.80 |
| $K_2O$ | <0.04 | <0.04 | <0.04 | <0.04 | 0.14 | <0.04 | <0.04 | 0.45 | <0.04 | <0.04 | 0.14 | <0.04 | 0.19 |
| NiO | 0.09 | 0.08 | <0.06 | <0.06 | <0.06 | <0.06 | <0.06 | 0.06 | <0.06 | <0.06 | <0.06 | <0.06 | 0.07 |
| Total | 99.6 | 99.6 | 99.0 | 99.5 | 99.7 | 98.4 | 100.1 | 99.5 | 98.8 | 99.7 | 99.1 | 98.4 | 100.4 |
| Mg# | 92.8 | 92.4 | 77.9 | 76.9 | 74.6 | 77.2 | 88.6 | 80.4 | 76.0 | 75.5 | 74.3 | 87.2 | 93.0 |
| Jd | 0.04 | 0.03 | 0.34 | 0.35 | 0.21 | 0.00 | 0.27 | 0.26 | 0.27 | 0.26 | 0.20 | 0.00 | 0.03 |
| Di + Hd | 0.78 | 0.79 | 0.51 | 0.51 | 0.62 | 0.84 | 0.62 | 0.56 | 0.66 | 0.65 | 0.63 | 0.87 | 0.82 |
| XsNa | 0.04 | 0.03 | 0.08 | 0.08 | 0.03 | 0.03 | | 0.02 | | | 0.03 | 0.04 | 0.02 |
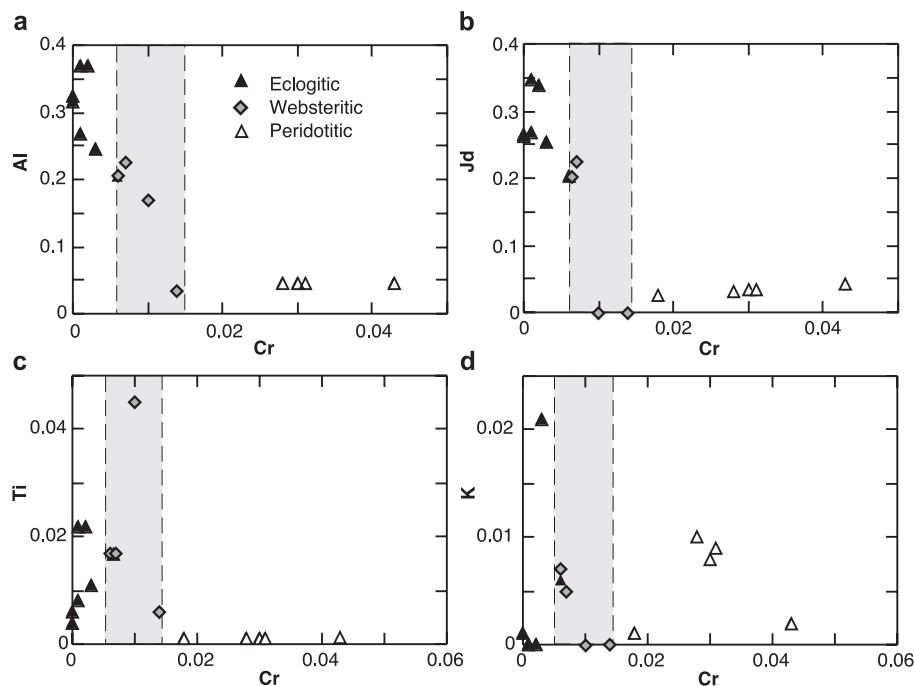
Fig. 4. Cation ratios (for six oxygen atoms) for eclogitic, websteritic (shaded area) and peridotitic clinopyroxene inclusions in diamond.

111H could be a result of metasomatic processes (e.g., Sobolev et al., 1998).

Potassium substitution in clinopyroxene is a function of increased formation pressure (Harlow and Veblen, 1991; Luth, 1997). In omphacite inclusions in eclogitic diamond, potassium contents typically range between 0.07 and 0.15 wt.% $K_2O$ (McCandless and Gurney, 1989). The potassium content of clinopyroxenes in the Buffalo Hills diamonds is variable ($< 0.04$ and 0.45 wt.%) and independent of composition and paragenesis (Fig. 4d). In one eclogitic diamond (111D), one omphacite inclusion is potassium-free, while another contains 0.45 wt.% $K_2O$. In a websteritic diamond (111H) containing both jadeite-rich and jadeite-free clinopyroxene, $K_2O$ is present in the jadeite-rich but not in the jadeite-free clinopyroxene. In addition, a peridotitic Cr-diopside contains 0.19 wt.% $K_2O$.

### 5.4. Olivine

Sixteen olivine inclusions were analysed from eight diamonds (representative analyses in Table 6). Forsterite contents range between 90.3 and 92.9, reflecting a mixture of diamonds from the harzburgitic

and lherzolitic parageneses (Meyer, 1987). The Mg# and abundances of Ca and Mn in lherzolitic olivine, including one from a diamond with coexisting garnet and clinopyroxene, suggest fertile compositions.

### 5.5. Chrome spinel

Six inclusions were extracted and analysed from a single diamond. Their compositions show some variation, the largest being in Mg# (52 to 59). Compared to chromite inclusions in diamonds from South Africa and Siberia, chromites in the Buffalo Hills diamond are more Fe-rich (mean Mg# = 58.2 versus 66 worldwide ($n$ = 156)). However, they are similar to chromites in diamonds from the Slave Craton (Mg# 56–64; Davies et al., 2004). The Cr# ($100Cr/(Cr + Al) = 86$) of these inclusions matches the average value of inclusions from diamond localities worldwide.

### 5.6. Ferropericlase

One ferropericlase inclusion was extracted from one diamond (Table 6). Ferropericlase is a phase formed from fertile peridotite at pressures and tem-

Table 6
Representative electron microprobe analyses of olivine (Fo) and a ferropericlase (fPer) inclusion

| Sample | 101 | 113 | 102B | 104A | 104B | 105B | 106C | K10 | K10 | 109A |
|--------|-----|-----|------|------|------|------|------|-----|-----|------|
| Mineral | Fo | Fo | Fo | Fo | Fo | Fo | Fo | Fo | Fo | fPer |
| Anal. | 3 | 4 | 2 | 4 | 3 | 3 | 3 | 2 | 2 | 3 |
| $SiO_2$ | 40.7 | 41.1 | 41.2 | 40.3 | 41.3 | 41.2 | 39.7 | 40.5 | 40.7 | <0.02 |
| $TiO_2$ | | | | | | | | | | 0.03 |
| $Al_2O_3$ | 0.02 | <0.02 | <0.02 | <0.02 | 0.02 | 0.02 | <0.02 | <0.02 | 0.02 | 0.21 |
| $Cr_2O_3$ | 0.08 | 0.05 | 0.12 | 0.07 | 0.07 | 0.06 | 0.08 | 0.09 | 0.05 | 1.00 |
| FeO | 7.23 | 7.88 | 7.06 | 8.30 | 7.45 | 7.76 | 8.10 | 9.55 | 8.50 | 20.0 |
| MnO | 0.08 | 0.09 | 0.06 | 0.15 | 0.12 | 0.10 | 0.10 | 0.10 | 0.15 | 0.22 |
| MgO | 51.3 | 50.7 | 51.6 | 50.3 | 51.1 | 50.5 | 50.9 | 49.7 | 50.1 | 75.8 |
| CaO | 0.06 | 0.05 | <0.03 | 0.09 | 0.03 | 0.10 | 0.05 | 0.11 | 0.09 | 0.01 |
| $Na_2O$ | | | | | | | | | | 0.50 |
| NiO | 0.33 | 0.37 | 0.34 | 0.41 | 0.34 | 0.38 | 0.36 | 0.38 | 0.44 | 1.43 |
| Total | 99.8 | 100.3 | 100.4 | 99.7 | 100.5 | 100.1 | 99.4 | 100.6 | 100.1 | 99.3 |
| Mg# | 92.7 | 92.0 | 92.9 | 91.5 | 92.4 | 92.1 | 91.8 | 90.3 | 91.3 | 87.1 |

peratures corresponding to the lower mantle (∼ 670 km; e.g., Ito and Takahashi, 1989), or in the upper mantle in conditions of low Si activity (Stachel et al., 1998, 2000). The Buffalo Hills ferropericlase has a composition typical of other ferropericlase inclusions in diamond of definite lower mantle origin, with respect to Mg#, Ni and Cr. In addition C-isotope ($\delta^{13}C = -4.6‰$) and IR-characteristics (Type II) of the diamond are typical of lower mantle diamonds. The occurrence of a diamond suite containing both ferropericlase and majoritic garnet inclusions draws parallel to other ultradeep (asthenosphere to lower mantle) diamond localities (e.g., Moore et al., 1991; Davies et al., 1999a; Harte et al., 1999; Hutchison et al., 1999; Kaminsky et al., 2000; Stachel et al., 2000). However, a second lower mantle phase to distinguish the paragenesis is lacking in this instance.

### 5.7. Rutile

Three large rutile inclusions of the eclogitic paragenesis were analysed from one diamond (111B). The inclusions contain trace amounts of FeO, $Cr_2O_3$, and $Al_2O_3$. In another diamond, a small rutile (not analysed) occurs in contact with eclogitic garnet and clinopyroxene.

### 5.8. Epigenetic inclusions

Epigenetic inclusions occurred as crack fillings and altered primary phases, consist dominantly of an assemblage of phlogopite, serpentine, Ca–Ti perovskite and carbonate. Analyses were carried out on polished mineral surfaces.

### 5.9. Geothermometry

Temperature calculations were carried out on eclogitic inclusions by the statistical approach of combining each discrete garnet inclusion ($n = 3$) with each clinopyroxene inclusion ($n = 2$) within a single eclogitic diamond (sample 108B). This procedure yielded a temperature of 1280 °C at a pressure of 5 GPa (Ellis and Green, 1979). In the same diamond, a garnet and clinopyroxene inclusion pair in mutual contact yields a slightly lower temperature for the same pressure value (1210 °C) indicating the inclusion pair re-equilibrated to lower temperatures during mantle storage. The temperature calculated from garnet and olivine in a lherzolitic diamond (sample K-10) is similar to the eclogitic diamond (1255 °C; O'Neill and Wood, 1979; assumed $P = 5$ GPa).

## 6. Carbon isotopes

On the basis of C-isotope values alone, and including the BH series of unknown paragenesis in Table 1, the Buffalo Hills diamonds cluster in three zones across a large range ($\delta^{13}C = -20.6‰$ to $-2.7‰$; Fig. 5). Most samples group around a peak with a typical average mantle value ($\delta^{13}C = -5$ av.), includ-
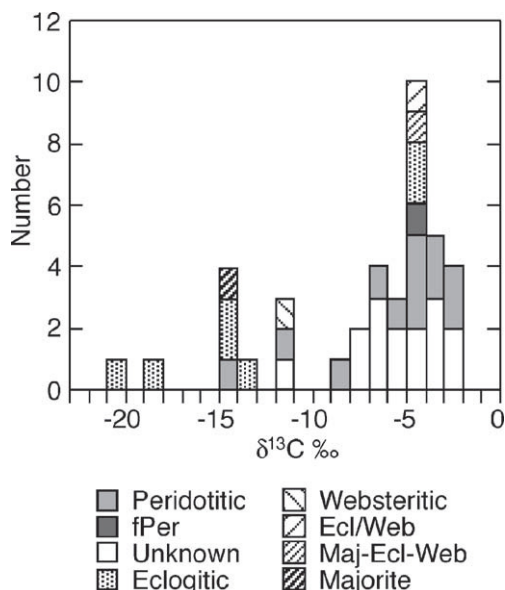
Fig. 5. Carbon isotopes and diamond parageneses.

ing diamonds containing ferropericlase, peridotitic, eclogitic and eclogitic + majoritic garnet + websteritic phases. Other diamonds with majoritic garnet, eclogitic, peridotitic and websteritic inclusions have intermediate compositions ($\delta^{13}C = -14.7$ to $-11.8$). Two eclogitic diamonds have the most $^{13}$C-depleted values ($\sim -20\permil$). From this data, we can link diamonds with eclogitic-majoritic garnet and websteritic inclusions into both the main and intermediate groups.

Two peridotitic diamonds and one websteritic diamond are $^{13}$C-depleted ($-14.6\permil$ and $-11.8\permil$), and lie outside the $\delta^{13}$C range of most peridotitic diamonds worldwide ($\delta^{13}C = -10\permil$ to $0\permil$; e.g., Kirkley et al., 1991). These compositions may indicate C-isotope heterogeneity in peridotitic mantle source. In view of the present inclusion mineralogy, they may also represent diamonds of mixed paragenesis, where the inclusions in the diamond were entrapped during growth in a peridotitic environment, while the bulk of the diamond grew at a different time in an eclogitic host rock with a $^{13}$C-depleted carbon source.

The large range in $^{13}$C-values in the Buffalo Hills eclogitic diamonds, which includes $^{13}$C-depleted compositions, is a feature seen in other eclogitic diamonds

globally. A simple explanation for this range is a source derivation from subducted ocean crust mixed with organic sedimentary material (e.g., Kirkley et al., 1991). An alternative model explains the range of $\delta^{13}$C values in eclogitic diamonds by Rayleigh fractionations through continuous extraction of mantle melts or fluids from the diamond source (Cartigny et al., 1998).

## 7. Nitrogen contents and nitrogen aggregation states

Nitrogen is the most common impurity in diamond and its substitution in kimberlitic diamonds is as high as 3000 ppm. The aggregation of nitrogen via diffusion in the diamond lattice is a time-temperature dependent process (Evans and Harris, 1989), but is influenced by the concentration of nitrogen, vacancies and by deformation. Because of the many factors that influence nitrogen aggregation in natural diamond, the thermal maturation histories cannot be accurately constrained by this method. Despite this limitation, FTIR-spectroscopy is a useful tool for characterising and comparing diamond groups of similar nitrogen defect characteristics relative to other diamonds from the same or related kimberlites.

From the 29 Buffalo Hills diamond set (Table 1), three groups are identified from their infrared spectral characteristics: (1) about 45% are nitrogen-free (Type II), (2) 33% have fully aggregated nitrogen defects (Type IaB) with platelet degradation and low to moderate nitrogen contents (65–830; av. 330 ppm-N), and (3) about 20% have low nitrogen aggregation states and moderate to high nitrogen contents (<30% IaB (aggregation from IaA to IaB); <1600 ppm-N). Type II diamonds (1) are grouped with (2) diamonds showing Type IaB characteristics because in most of the Type IaB diamonds nitrogen occurs in low amounts. The occurrence of pure IaB defects suggests that the diamonds were affected by storage in the mantle at high temperatures, for a significant residence time, and/or with significant strain. Strong deformation evident in many of these diamonds suggests the high degrees of nitrogen aggregation could reflect this process. The occurrence of such a high proportion of Type II and pure IaB diamonds with degraded platelets is rare in diamond populations
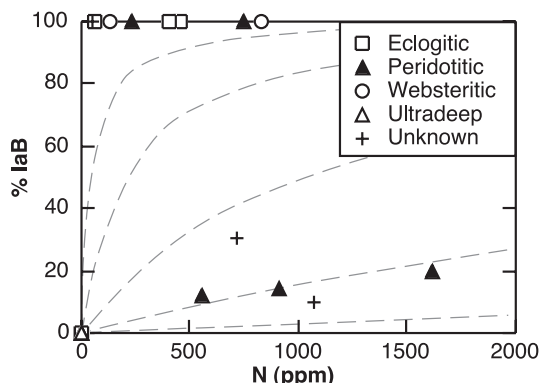
Fig. 6. Relationships between nitrogen contents, nitrogen aggregation states and inclusion parageneses in the Buffalo Hills diamonds from this study. The dashed isochron–isotherm lines define areas of similar nitrogen contents and aggregation states, inferring similar temperature/time/deformation histories (e.g., Evans and Harris, 1989).

worldwide and is in contrast to Type I diamonds from the Slave Craton with unusually low nitrogen aggregation states (Stachel et al., 2003; Davies et al., 2004). The Type IaA–IaB diamond group witnessed a different mantle storage history. These diamonds experienced shorter or cooler mantle storage conditions. Half of these diamonds also show strong deformation features.

Diamonds from all parageneses in this study are represented in the Type II and IaB IR-group (eclogitic, peridotitic, websteritic, and diamonds containing ferropericlase and majoritic garnet). The Type I diamonds with lower nitrogen aggregation states are peridotitic and have average mantle C-isotope values (Fig. 6).

## 8. Discussion

Mineral inclusion data from the Buffalo Hills diamonds suggest that the diamonds grew in host rocks of changing bulk chemistry and pressure (depth). These changes are recorded in the highly variable Cr, Na and K contents in clinopyroxenes, majoritic garnet, with compositions indicating formation at high pressure in the asthenosphere, and eclogitic and websteritic inclusions in single diamonds. Additional evidence for diamond growth in various and changing chemical environments comes from variable Cr-spinel compositions in a single diamond, and a diamond containing ferropericlase indicating a possible lower mantle origin. Compositional differences between isolated minerals in single diamonds could indicate diamond growth in a metasomatic environment (Sobolev et al., 1998). However, the occurrence of majoritic garnet with eclogitic and websteritic phases in a single diamond rules out this possibility.

Carbon isotope compositions show considerable overlap in diamonds containing eclogitic, peridotitic, websteritic, asthenospheric and ferropericlase inclusions. These diamond types are spread across two of three clusters in the $\delta^{13}C$ distribution ($-20.6‰$ to $-2.7‰$). Morphological and IR-characteristics also do not conform to paragenetic groupings. These lines of evidence support the proposal that diamond growth occurred in a dynamic mantle environment (Davies et al., 1999b; Taylor et al., 1999).

### 8.1. A model

The combined mineral inclusion, nitrogen content and aggregation state and C-isotope data provides evidence for at least two generations of diamond growth beneath the Buffalo Head terrane. (1) Type II diamonds containing majoritic garnet and ferropericlase formed in the asthenosphere and possibly the uppermost lower mantle, respectively, and were subsequently transported to the base of the lithosphere. Here, Type II and Type I diamonds crystallised or continued to grow from fluids in peridotitic and eclogitic mantle material.

Mechanisms by which diamonds are transported from the asthenosphere and lower mantle to the lithosphere could be by either mantle convection (Stachel et al., 2003), an ascending plume (Davies et al., 1999a) or in deep-seated proto-kimberlite melts. The interaction of small volume melts with eclogitic and peridotitic rocks may have promoted diamond growth in fluids and produced the intermediate websteritic inclusion compositions, and the overlap in C-isotope values between eclogitic, peridotitic, websteritic, asthenospheric and ultradeep? diamonds (e.g., Wang, 1998). Dynamic transport of diamond at high T can explain the strong deformation and the extremely high nitrogen aggregation states. (2) A second generation of diamonds with Type IaA–IaB nitrogen

aggregation, high nitrogen contents and peridotitic inclusions do not show evidence of dynamic mantle growth histories except for strong plastic deformation in some stones. These diamonds are likely to have crystallised in a cooler mantle, and possibly at a later time, at the base of the cratonic lithosphere. The two groups of diamonds were later sampled and emplaced at the Earth's surface in kimberlite magmas.

## Acknowledgements

## References

Carlson, S.M., Hillier, W.D., Hood, C.T., Pryde, R.P., Skelton, D.H., 1998. The Buffalo Hills kimberlites: a newly-discovered diamondiferous kimberlite province in North-Central Alberta, Canada. Proc. 7th Internat. Kimberlite Conf. Red Roof Designs, Cape Town, pp. 109–116.

Cartigny, P., Harris, J.W., Javoy, M., 1998. Eclogitic diamond formation at Jwaneng: no room for a recycled component. Science 280, 1421–1424.

Davies, R.M., Griffin, W.L., O'Reilly, S.Y., 1999a. Diamonds from the deep: pipe DO27, Slave craton, Canada. Proc. 7th Internat. Kimberlite Conf. Red Roof Designs, Cape Town, pp. 148–155.

Davies, R.M., Griffin, W.L., O'Reilly, S.Y., 1999b. Growth structures and nitrogen characteristics of Group B diamonds from Wellington and Bingara, eastern Australia. Proc. 7th Internat. Kimberlite Conf. Red Roof Designs, Cape Town, pp. 156–163.

Davies, R.M., Griffin, W.L., O'Reilly, S.Y., Doyle, B.J., 2004. Mineral inclusions and geochemical characteristics of microdiamonds from the DO27, A154, A21, A418, DO18, DD17 and Ranch Lake kimberlites at Lac de Gras, Slave Craton, Canada. Lithos 77, 39–55 this volume [doi:10.1016/j.lithos.2004.016].

Ellis, D.J., Green, D.H., 1979. An experimental study of the effect of Ca upon garnet-clinopyroxene Fe–Mg exchange equilibria. Contrib. Mineral. Petrol. 71, 13–22.

Evans, T., Harris, J.W., 1989. Nitrogen aggregation, inclusion equilibration temperatures and the age of diamonds. In: Ross, J., et al., (Eds.), Kimberlites and Related Rocks v.2. Their Mantle/Crust Setting. Spec. Publ. Geol. Soc. Aust., vol. 14, pp. 1002–1006.

Griffin, W.L., Shee, S.R., Ryan, C.G., Win, T.T., Wyatt, B.A., 1999. Harzburgite to lherzolite and back again: metasomatic processes in ultramafic xenoliths from Wesselton kimberlite, Kimberly, South Africa. Contrib. Mineral. Petrol. 134, 232–250.

Hall, A.E., Smith, C.B., 1984. Lamproite diamonds—are they different? In: Glover, J.E., Harris, P.G. (Eds.), Kimberlite Occurrence and Origin. Publ. Univ.West. Aust., Geol. Dept., vol. 8, pp. 167–212.

Harlow, G.E., Veblen, D.R., 1991. Potassium in clinopyroxene inclusions from diamond. Science 251, 652–655.

Harte, B., Harris, J.W., Hutchison, M.T., Watt, G.R., Wilding, M.C., 1999. Lower mantle mineral associations in diamonds from Sao Luiz, Brazil. In: Fei, Y., Bertka, C.M., Mysen, B.O. (Eds.), Mantle Petrology: Field Observations and High Pressure Experimentation: A tribute to Francis R. (Joe) Boyd. Spec. Publ.-Geochem. Soc., vol. 6, pp. 125–153.

Hutchison, M.T., Cartigny, P., Harris, J.W., 1999. Carbon and nitrogen compositions and physical characteristics of transition zone and lower mantle diamonds from Sao Luiz, Brazil. Proc. 7th Internat. Kimberlite Conf. Red Roof Designs, Cape Town, pp. 372–382.

Irifune, T., Hibberson, W.O., Ringwood, A.E., 1986. Eclogite–garnetite transformations at high pressure and its bearing on the occurrence of garnet inclusions in diamond. In: Ross, J., et al., (Eds.), Kimberlites and Related Rocks v. 2. Their Mantle/Crust Setting. Spec. Publ. Geol. Soc. Aust., vol. 14, pp. 877–882.

Ito, E., Takahashi, E., 1989. Postspinel transformations in the system $Mg_2SiO_4$–$Fe_2SiO_4$ and some geophysical implications. J. Geophys. Res. 94, 10637–10646.

Jaques, A.L., Hall, A.E., Sheraton, J.W., Smith, C.B., Sun, S.-S., Drew, R.M., Foudoulis, C., Ellingsen, K., 1989. Composition of crystalline inclusions and C-isotope composition of Argyle and Ellendale diamonds. In: Ross, J., et al., (Eds.), Kimberlites and Related Rocks v. 2. Their Mantle/Crust Setting. Spec. Publ. Geol. Soc. Aust., vol. 14, pp. 966–989.

Kaminsky, F.V., Zakharchenko, O.D., Davies, R.M., Griffin, W.L., Khachatryan-Blinova, G.K., Shiryaev, A.A., 2000. Superdeep diamonds from the Juina Area, Mato Grosso State, Brazil. Contrib. Mineral. Petrol. 140, 734–753.

Kirkley, M.B., Gurney, J.J., Otter, M.L., Hill, S.J., Daniels, L.R., 1991. The application of C isotope measurements to the identification of the sources of C in diamonds: a review. Appl. Geochem. 6, 477–494.

Luth, R.W., 1997. Experimental study of the system phlogopite–diopside from 3.5 to 17 GPa. Am. Mineral. 82, 1198–1209.

McCandless, T.E., Gurney, J.J., 1989. Sodium in garnet and potassium in clinopyroxene: criteria for classifying mantle eclogites. Internal Rept. 10, August 1986, KRG, Univ. Cape Town.

McNicoll, V.J., Theriault, R.J., McDonough, M.R., 2000. Taltson basement gneissic rocks: U–Pb and Nd isotopic constraints on the basement to the Paleoproterozoic Taltson magmatic zone, northeastern Alberta. Can. J. Earth Sci. 37, 1475–1596.

Mendelssohn, M.J., Milledge, H.J., 1995. Geologically significant

information from routine analysis of the mid-infrared spectra of diamonds. Int. Geol. Rev. 37, 95–110.

Meyer, H.O.A., 1987. Inclusions in diamond. In: Nixon, P.H. (Ed.), Mantle Xenoliths. John Wiley and Sons, New York, pp. 501–522.

Moore, R.O., Gurney, J.J., Fipke, C.E., 1989. The development of advanced technology to distinguish between diamondiferous and barren diatremes. Geol. Surv. Canada Open File Rept. 2124, 4 vols.

Moore, R.O., Gurney, J.J., Griffin, W.L., Shimuzu, N., 1991. Ultra-high pressure garnet inclusions in Monastery diamonds: trace element abundance patterns and conditions of origin. Eur. J. Mineral. 3, 213–230.

Norman, M.D., Pearson, N.J., Sharma, A., Griffin, W.L., 1996. Quantitative analysis of trace elements in geological materials by laser ablation ICPMS: instrumental operating conditions and calibration values of NIST glasses. Geostand. Newsl. 20, 247–261.

Norman, M.D., Griffin, W.L., Pearson, N.J., Garcia, M.O., O'Reilly, S.Y., 1998. Quantitative analysis of trace element abundances in glasses and minerals: a comparison of laser ablation ICPMS, solution ICPMS, proton microprobe, and electron microprobe data. J. Anal. At. Spectrom. 13, 477–482.

O'Neill, H.S.C., Wood, B.J., 1979. An experimental study of Fe–Mg partitioning between garnet and olivine and its calibration as a geothermometer. Contrib. Mineral. Petrol. 70, 59–70.

Robinson, D.N., Scott, J.A., Van Niekerk, A., Anderson, V.G., 1989. The sequence of events reflected in the diamonds of some southern African kimberlites. In: Ross, J., et al., (Eds.), Kimberlites and Related Rocks v.2. Their Mantle/Crust Setting. Spec. Publ. Geol. Soc. Aust., vol. 14, pp. 990–1000.

Ross, G.M., 2002. Introduction to special issue of Canadian Journal of Earth Sciences: the Alberta Basement Transect of Lithoprobe. Can. J. Earth Sci. 39, 287–288.

Ross, G.M., Parrish, R.R., Villeneuve, M.E., Bowring, S.A., 1991. Geophysics and geochronology of the crystalline basement of the Alberta Basin, western Canada. Can. J. Earth Sci. 28, 512–522.

Sobolev, N.V., Galimov, E.M., Smith, C.B., Yefinova, E.S., Maltsev, K.A., Hall, A.E., Usova, L.V., 1986. Comparative characteristics of morphology, inclusions and carbon isotope composition of diamonds in alluvial deposits of the King George River and lamproite deposits of Argyle. Geol. Geofiz. 12 (in Russ.).

Sobolev, N.V., Snyder, G.A., Taylor, L.A., Keller, R.A., Yefimova, E.S., Sobolev, V.N., Shimizu, N., 1998. Extreme chemical diversity in the mantle during eclogitic diamond formation: evidence form 35 garnet and 5 pyroxene inclusions in a single diamond. Int. Geol. Rev. 40, 567–578.

Stachel, T., Harris, J.W., Brey, G.P., 1998. Rare and unusual mineral inclusions in diamonds from Mwadui, Tanzania. Contrib. Mineral. Petrol. 132, 34–47.

Stachel, T., Harris, J.W., Brey, G.P., Joswig, W., 2000. Kankan diamonds (Guinea): II. Lower mantle inclusion parageneses. Contrib. Mineral. Petrol. 140, 16–27.

Stachel, T., Harris, J.W., Tappert, R., Brey, G.P., 2003. Peridotitic diamonds from the Slave and the Kaapvaal cratons—similarities and differences based on a preliminary data set. Lithos 71, 489–503.

Taylor, L.A., Snyder, G.A., Camacho, A., 1999. Diamond: just another metamorphic mineral? Abst. 9th Ann. Goldschmidt Conf., LPI Contribution No. 971, Lunar and Planetary Institute, Houston, pp. 291–292.

Villeneuve, M.E., Ross, G.M., Parrish, R.R., Therault, T.J., Miles, W., Broome, J., 1993. Geophysical subdivision, U–Pb geochronology and Sm–Nd isotope geochemistry of the crystalline basement of the Western Canada sedimentary Basin, Alberta and northeastern British Columbia. Bull. Geol. Surv. Can. 447, p. 85.

Wang, W., 1998. Formation of diamond with mineral inclusions of "mixed" eclogite and peridotite paragenesis. Earth Planet. Sci. Lett. 160, 831–843.

Woods, G.S., Purser, G.C., Mtimkulu, S.S., Collins, A.T., 1990. The nitrogen content of Type Ia natural diamonds. Phys. Chem. Solids 51, 1191–1197.